

In situ monitoring of a flash light sintering process using silver nano-ink for producing flexible electronics

This article has been downloaded from IOPscience. Please scroll down to see the full text article.

2013 Nanotechnology 24 035202

(<http://iopscience.iop.org/0957-4484/24/3/035202>)

View [the table of contents for this issue](#), or go to the [journal homepage](#) for more

Download details:

IP Address: 166.104.17.11

The article was downloaded on 23/12/2012 at 07:33

Please note that [terms and conditions apply](#).

In situ monitoring of a flash light sintering process using silver nano-ink for producing flexible electronics

Wan-Ho Chung¹, Hyun-Jun Hwang¹, Seung-Hyun Lee² and Hak-Sung Kim^{1,3}

¹ School of Mechanical Engineering, Hanyang University, 17 Haendang-Dong, Seongdong-Gu, Seoul 133-791, Korea

² Department of Printed Electronics, Korea Institute of Machinery and Materials 156, Gajungbuk No, Yuseong-Gu, Deajeon, 305-343, Korea

³ Institute of Nano-Science and Technology, Hanyang University, 17 Haendang-Dong, Seongdong-Gu, Seoul 133-791, Korea

E-mail: kima@hanyang.ac.kr

Received 2 October 2012, in final form 20 November 2012

Published 21 December 2012

Online at stacks.iop.org/Nano/24/035202

Abstract

In this work, a flash light sintering process using silver nano-inks is investigated. A silver nano-ink pattern was printed on a flexible PET (polyethylene terephthalate) substrate using a gravure-offset printing system. The printed silver nano-ink was sintered at room temperature and under ambient conditions using a flash of light from a xenon lamp using an in-house flash light sintering system. In order to monitor the light sintering process, a Wheatstone bridge electrical circuit was devised and changes in the voltage difference of the silver nano-ink were recorded during the sintering process using an oscilloscope. The sheet resistance changes during the sintering process were monitored using the *in situ* monitoring system devised, under various light conditions (e.g. light energy, on-time and off-time duration, and pulse numbers). The microstructure of the sintered silver film and the interface between the silver film and the PET substrate were observed using a scanning electron microscope, a focused ion beam and an optical microscope. The electrical sheet resistances of the sintered silver films were measured using a four-point probe method. Using the *in situ* monitoring system devised, the flash light sintering mechanism was studied for each type of light pulse (e.g. evaporation of organic binder followed by the forming of a neck-like junction and its growth, etc).

The optimal flash light sintering condition is suggested on the basis of the *in situ* monitoring results. The optimized flash light sintering process produces a silver film with a lower sheet resistance (0.95 Ω /sq) compared with that of the thermally sintered silver film (2.03 Ω /sq) without damaging the PET substrate or allowing interfacial delamination between the silver film and the PET substrate.

(Some figures may appear in colour only in the online journal)

1. Introduction

Recently, printing electronics has been studied as an alternative to the standard method of production of electronic devices. Electronic components printed using metal nano-ink have been used in various applications such as flexible radio

frequency identification (RFID) tags, flexible organic light emitting diodes (OLED), and wearable electronics [1]. Metal nano-ink made from Au, Ag and Cu nanoparticles is printed onto a flexible polymer substrate using non-contact printing processes such as ink-jet printing and roll-to-roll printing processes such as gravure, the gravure-offset method and

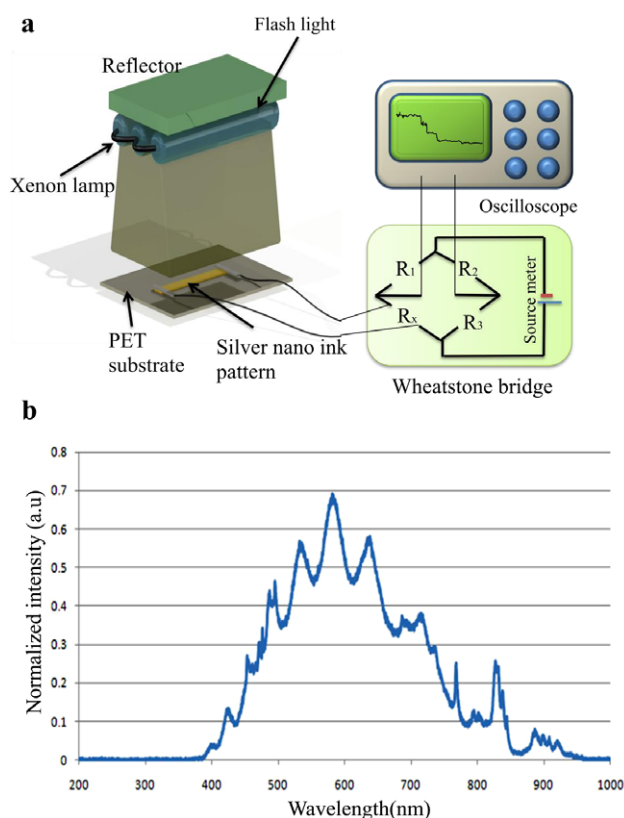


Figure 1. (a) Schematic diagrams of the flash light sintering and the *in situ* monitoring. (b) Spectral distribution of a xenon flash lamp.

the flexo-graph method [2]. In particular, the gravure-offset printing method has been adopted for producing plasma display panels (PDP) electrodes, EMI (electromagnetic interference) mesh filters and touch screen electrodes. If the gravure-offset printing process is combined with a roll-to-roll process, it is very cost effective for the mass production of printed electronics [23]. Printed metal nano-inks are then sintered using thermal heating, electrical, laser, or microwave sintering techniques [3–10]. Thermal sintering conducted at a high temperature (150–300 °C) over long times (30–60 min) may result in damage to vulnerable substrates. For this reason, the thermal method is not appropriate for use with flexible substrates such as PET, PEN (polyethylene naphthalate), and paper.

In contrast, laser sintering requires only a short sintering time at a low temperature and does not damage the substrate [7]. However, laser sintering has a small local sintering area and requires a sophisticated system. The electrical sintering method is also complicated due to the high voltage and current levels flowing through the nanopatterns [8]. To resolve these problems, the flash light sintering method was suggested in our previous studies [11–20]. In this method, a flash light from a xenon lamp is used for the sintering of metal nano-inks. Using white flash light irradiation, nanoparticles can be sintered in a few milliseconds at room temperature under ambient conditions. Meanwhile, the mechanism of sintering of silver nanoparticles using a thermal method has been

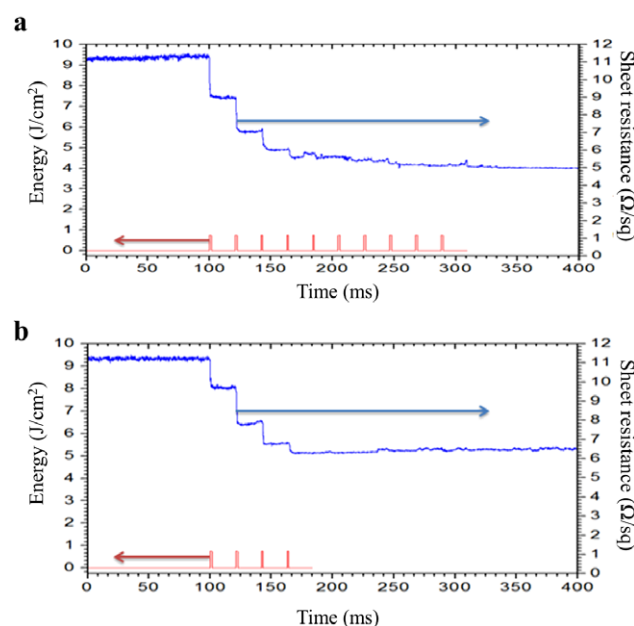


Figure 2. Comparison of the cases for pulse number 10 and 4 (energy: 0.75 J cm^{-2} per pulse). (a) *In situ* monitoring result for the ten-pulse case. (b) *In situ* monitoring result for the four-pulse case.

studied through spectroscopic ellipsometry [5]. However, the mechanism of sintering of silver nanoparticles in a brief (a few milliseconds) flash light sintering process has not been studied in depth. To investigate the flash light sintering mechanism, the monitoring of the flash light sintering process in real time should be performed.

In this work, in order to monitor the flash light sintering process over a few milliseconds, a Wheatstone bridge electrical circuit was devised and the resistance changes in the silver nanopatterns were recorded using an oscilloscope during the sintering process. The microstructure of the sintered silver film and the interface between the silver film and the PET substrate were investigated using a scanning electron microscope (SEM), a focused ion beam (FIB), and an optical microscope.

2. Experiment details

2.1. Specimen preparation

Silver nano-ink (ANP GDP-OS(12000)) was printed on flexible polyethylene terephthalate (PET) substrate (SKC SH34 thickness: $100 \mu\text{m}$) under ambient conditions using a roll-to-roll gravure-offset printing system [24]. The operating printing speed was set to 0.6 m min^{-1} and the printing force was set to 15 kgf. The silver nano-ink was composed of 66.56 wt% silver nanoparticles ranging from 30 to 50 nm in size, 30–33 wt% solvent, and 2–3 wt% polymer. The solvent used on the silver nano-ink was made up of α -terpinol (alpha-terpinol) and BCA (diethylene glycol monobutyl acetate). The silver nano-ink polymer was a polymeric resin. The viscosity was 12 427 cps at 0.4 rpm shear rate, which was measured using Brookfield viscometry with a CP51 spindle.

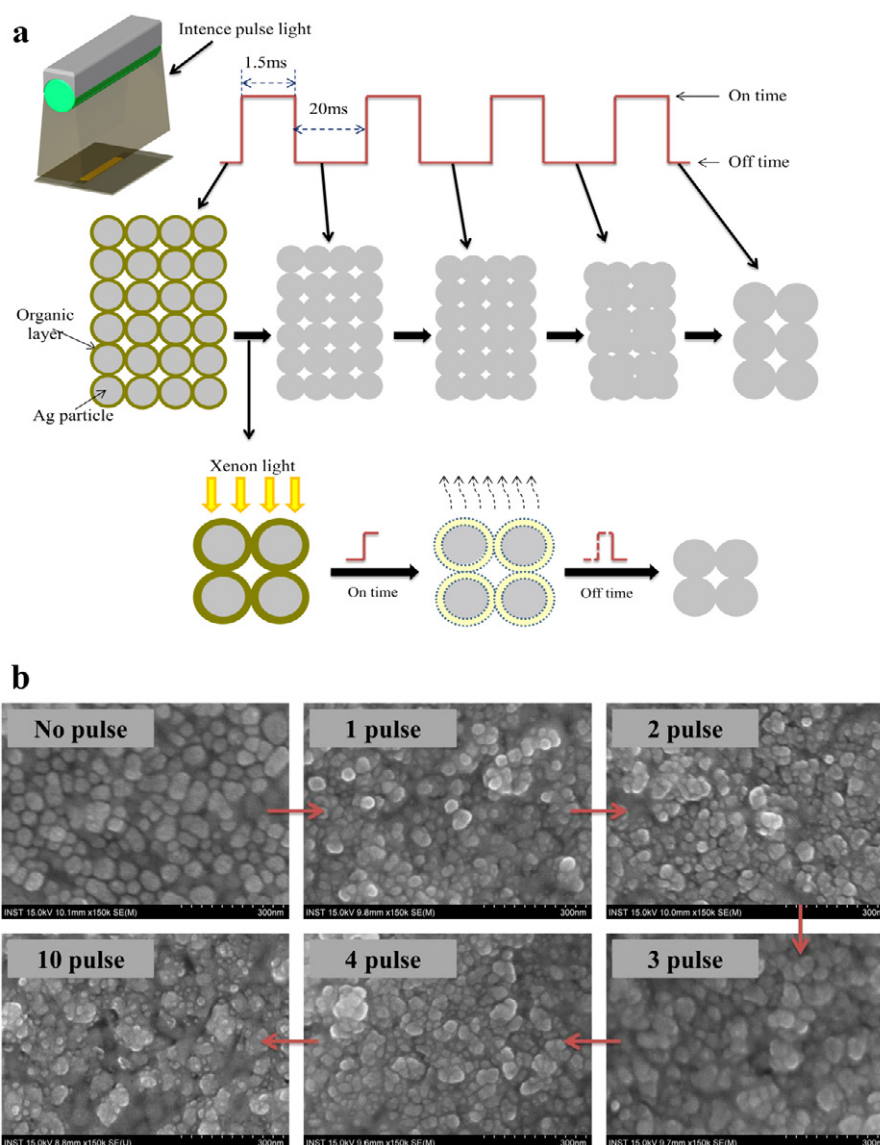


Figure 3. (a) Schematic diagrams for the sintering processes for silver nanoparticles, for different pulse numbers. (b) The silver nano-inks sintered by using the flash light, and the SEM images of silver nanoparticles sintered using different pulse numbers.

The size of the pattern was 30 mm (length) \times 3 mm (width). The printed pattern was dried by using a thermal dryer for about 2–3 min. After the drying process, the initial thickness of the printed film was about 400 nm.

2.2. The thermal sintering process

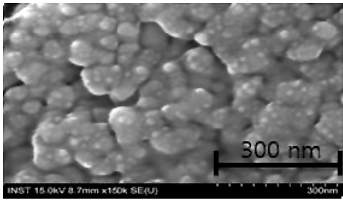
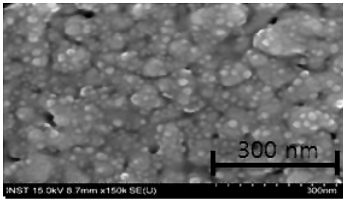
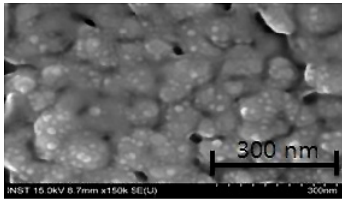
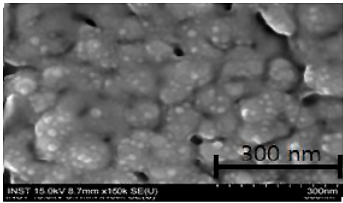
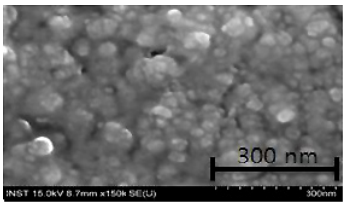
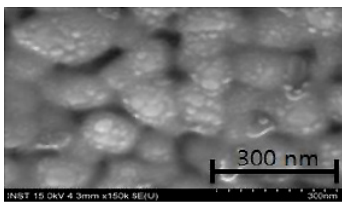
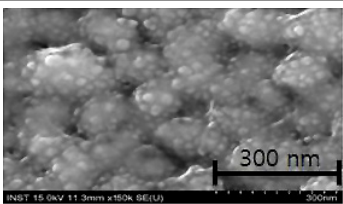
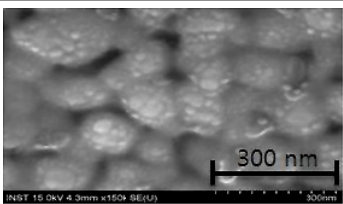
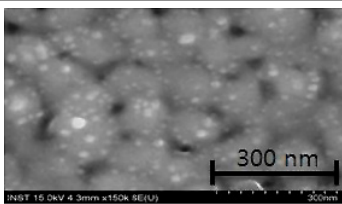
In order to thermally sinter the silver nano-ink, an electrical furnace (FH-05, Daihan Scientific) was used. The silver nano-inks were thermally sintered at temperatures ranging from 80 to 150 °C for 1 h to avoid damaging the PET substrate.

2.3. The flash light sintering process

For the sintering of the silver nano-ink, an in-house flash light sintering system was assembled, and this included a

xenon lamp (Perkin-Elmer Co.), a power supply, capacitors, a pulse controller, and a reflector [11]. In the in-house flash light sintering system, arc plasma was generated in the xenon lamp by applying high electrical current. The xenon lamp then emitted white light over a wide range of wavelengths from 380 to 950 nm (figure 1(b)). Our flash light sintering system was designed to supply 99 maximum shots and 100 J cm⁻² maximum energy on a millisecond scale with a minimum pulse interval of 1 ms by controlling the electrical current and voltage [12]. The nanosilver films were placed at a distance of 3 mm from the flash lamp. The printed nanosilver patterns were irradiated with flashes of light with varying irradiation energy (from 0.75 to 3.5 J cm⁻²), pulse duration (from 1.5 to 6 ms), time interval (from 20 to 0 ms) between pulses, and pulse number.

Table 1. *In situ* monitoring results and SEM images for (a) off-time 10, 5 and 0 ms cases, (b) on-time 6, 4 and 1.5 ms cases, (c) energy 2.5, 3 and 3.5 J cm⁻² cases.

	10 ms	5 ms	0 ms
Off-time			
	(a)	(b)	(c)
	6 ms	4 ms	1.5 ms
On-time			
	d	e	f
	2.5 J cm ⁻²	3 J cm ⁻²	3.5 J cm ⁻²
Energy			
	g	h	i

2.4. *In situ* monitoring of flash light sintering phenomena

In this study, in order to monitor a light sintering process with a duration of a few milliseconds, a Wheatstone bridge electrical circuit was devised using a source meter (2611A, Keithley). The changes in the voltage differential applied to the silver nanopatterns were recorded using an oscilloscope (DL1740E, Yokogawa) at 20×10^4 samples per second during the sintering process (figure 1(a)) [8]. The source meter was used to apply a constant voltage (4 V) and current (1.2 A) to the Wheatstone bridge circuit. In the Wheatstone bridge circuit, the values of the resistances R_1 , R_2 and R_3 were fixed at 1 Ω . The voltage difference (V_D) between the two middle points of the Wheatstone bridge was measured and recorded using an oscilloscope (see figure 1(a)). From the voltage difference (V_D), the unknown resistance could be calculated using the following equation:

$$R_x = V_I + 2V_D/V_I - 2V_D \quad (1)$$

where R_x is the sheet resistance of the silver nanopattern, V_I is the input voltage (4 V) of the Wheatstone bridge, and V_D is the voltage difference of the Wheatstone bridge.

2.5. Characterization

The microstructure of the silver film and the interface between the silver film and the PET substrate were observed using

a scanning electron microscope (SEM, S4800, Hitachi), focused ion beam (FIB), and optical microscope (BX51M, Olympus). The electrical sheet resistances of the sintered silver films were measured using a four-point probe method.

3. Results and discussion

For the sintering of silver nanoparticles, a flash of light was emitted as several separate pulses from the xenon lamp. Figure 2 shows the *in situ* monitoring results when the flash light (on-time: 1.5 ms, off-time: 20 ms, irradiation energy per pulse: 0.75 J cm⁻²) was applied. As shown in figures 2(a) and (b), it was observed that the sheet resistance decreased incrementally at each flash light pulse. The sheet resistance decreased significantly after the first pulse, and this was followed by a larger drop in sheet resistance after the second pulse. After the third pulse, the magnitude of the drop in sheet resistance declined, and the sheet resistance stabilized at its final value (6.5 Ω /sq). It appeared that the sintering of silver nanopatterns continued during pulse irradiation up to the fourth pulse; however, after the fourth pulse of irradiation, sintering did not occur. As shown in figure 2(b), the trend in the change in resistance in the four-pulse case was similar to that of the previous condition (ten pulses).

During the sintering process, the morphology of the silver nanoparticles changed, as shown in the scanning electron

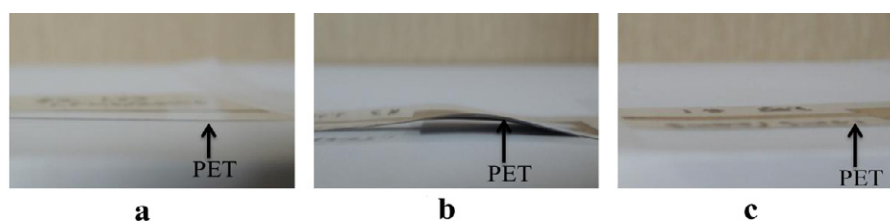


Figure 4. The photo camera image of the PET substrate (a) before sintering, and after sintering: (b) energy: 0.75 J cm^{-2} , pulse number: 10; (c) energy: 0.75 J cm^{-2} , pulse number: 4.

microscope (SEM) micrographs (figure 3(b)). The grain size of the silver nanoparticles increased with pulse number up to the fourth pulse. During first light irradiation, it appeared that the organic layer surrounding the silver nanoparticles was removed and slight necking connections were formed (see figure 3(a)). This necking formation during the first pulse might decrease the sheet resistance of the silver nano-ink pattern (see figure 2(a)). During the second flash, the necking connections between the silver nanoparticles became denser, which might account for the larger drop in sheet resistance compared with the first drop (see figures 2(a) and 3(a)). The third and fourth flashes caused denser and closer neck junctions to be formed among the silver nanoparticles, which caused the observed third and fourth drops in sheet resistance (see figure 3(a)). However, growth of the necking structures did not occur after the fourth pulse, possibly because the grain size of the silver nanoparticles had reached its maximum. This is consistent with the result of the sheet resistance measurement, in which the sheet resistance did not decrease after the fourth pulse (figure 2(a)).

Pulses with an irradiation energy of 0.75 J cm^{-2} were used to sinter the silver patterns, and the images of the specimens were recorded using a digital camera (D7000, Nikon). As shown in figure 4(b), after ten pulses of irradiation for the silver patterns, the PET substrate was damaged and deformed. However, degradation of the PET substrate was not observed after four pulses of irradiation, as shown in figure 4(c). Therefore, it can be deduced that excessive irradiation with the flash light (after four pulses) can degrade the PET substrate and cause damage (see figure 2(a)). Thus, no more than four pulses were used in subsequent experiments so as not to damage the PET substrate.

The interval time (off-time) between pulses was varied and its effect on the sintering was investigated. The pulse energy and the number of pulses were fixed at 0.75 J cm^{-2} and four pulses, respectively. In order to analyze the effects of interval time (off-time), flashes of light with off-times of 20, 10, 5, and 0 ms were used, and the resulting sheet resistance changes were monitored. As shown in figures 5(e) and (a)–(c), the sheet resistance of the sintered silver nano-ink decreased with off-time from 20 to 0 ms. In addition, connections between silver nanoparticles became more common as the off-time decreased, as shown in the SEM images in tables 1(a)–(c). In the case of an off-time of 0 ms, the four pulses were merged into a single pulse. This single-pulse condition resulted in better conductivity than for any other condition that did deform the PET substrate.

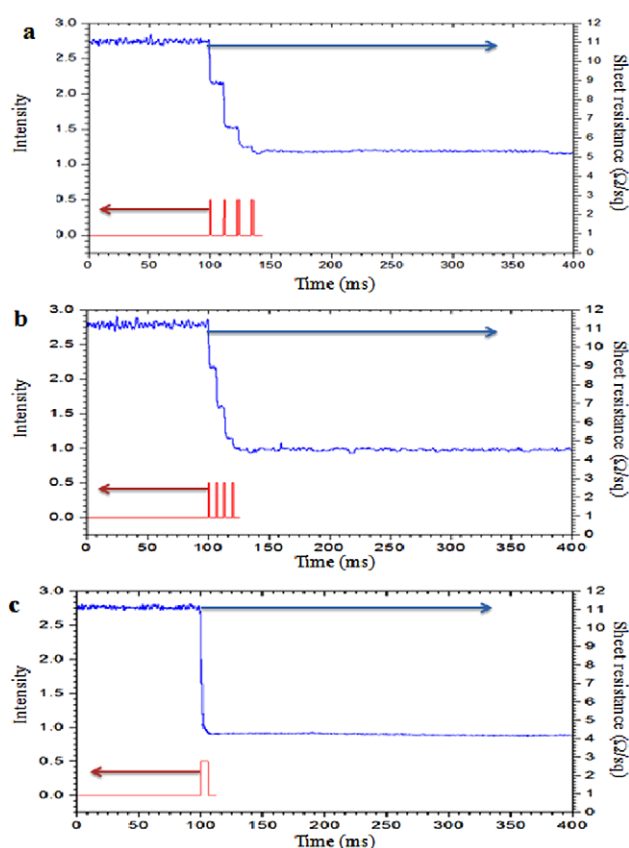


Figure 5. *In situ* monitoring results and SEM images for off-time 10, 5 and 0 ms. (a) *In situ* monitoring result for the off-time 10 ms case. (b) *In situ* monitoring result for the off-time 5 ms case. (c) *In situ* monitoring result for the off-time 0 ms case.

In order to determine the optimal on-time for sintering, on-times of 6, 4, and 1.5 ms with a fixed irradiation energy of 3 J cm^{-2} were tested. The resistance changes are shown in figures 6(a)–(c) as a function of on-time. The sheet resistance decreased with decreasing on-time. The gradual growth of neck-like junctions among the silver nanoparticles was observed, as shown in the SEM images (tables 1(d)–(f)). The connections between silver nanoparticles were perfectly formed in the case of 1.5 ms of on-time. On the basis of the results of previous experiments, these connections between nanoparticles are closely associated with the sheet resistance of silver nano-ink patterns.

In order to optimize the energy per pulse for sintering silver patterns, changes in the resistances of the silver patterns during sintering processes with different irradiation energies

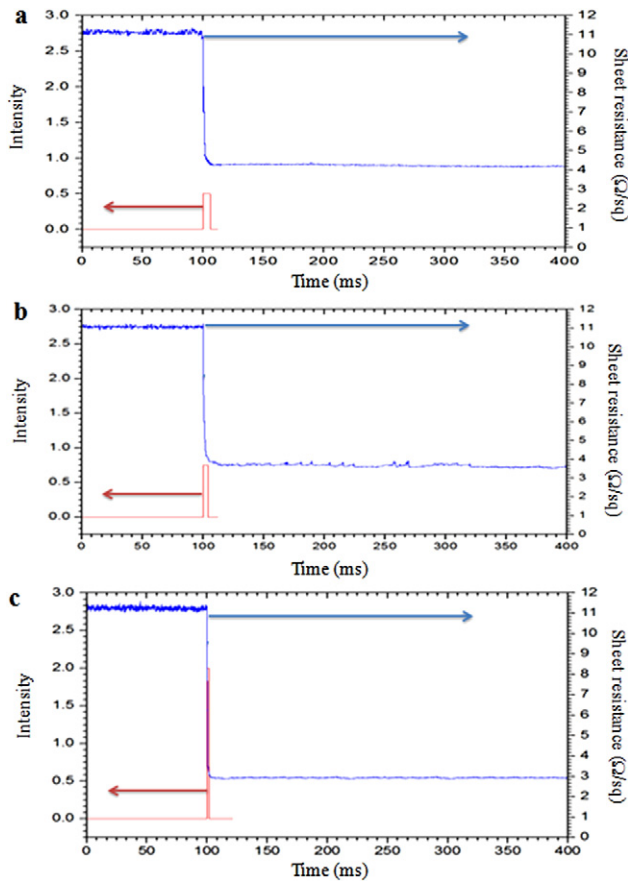


Figure 6. *In situ* monitoring results and SEM images for on-time 6, 4 and 1.5 ms. (a) *In situ* monitoring result for the on-time 6 ms case. (b) *In situ* monitoring result for the on-time 4 ms case. (c) *In situ* monitoring result for the on-time 1.5 ms case.

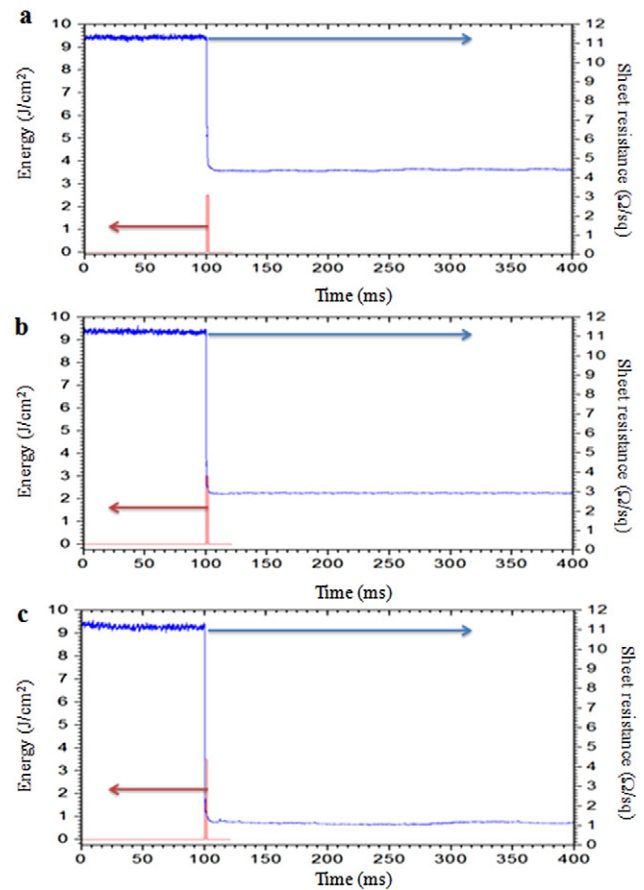


Figure 7. *In situ* monitoring results and SEM images for the energy 2.5, 3 and 3.5 J cm⁻² cases. (a) *In situ* monitoring result for energy 2.5 J cm⁻². (b) *In situ* monitoring result for energy 3 J cm⁻². (c) *In situ* monitoring result for energy 3.5 J cm⁻².

(2.5, 3 and 3.5 J cm⁻²) were tested (figures 7(a)–(c)). As shown in these figures, the sheet resistance decreased with increasing pulse energy. The SEM images of the flash light sintered silver nanoparticles show that connections developed between the silver nanoparticles and the grain size of the particles became larger with increasing pulse energy (tables 1(g)–(i)). The sheet resistance of the silver patterns sintered at 3.5 J cm⁻² pulse energy was also lower than with any other condition. However, interfacial delamination between the silver film and the PET substrate occurred above a pulse energy of 3.5 J cm⁻², as shown in the FIB images (figures 8(c) and (f)), because the high light energy intensity damaged the PET substrate. The optimally sintered silver pattern (on-time 1.5 ms, off-time 0 ms, one pulse and 3 J cm⁻² per pulse) shows coarse grains and a smooth interface with the PET substrate. The surface of the unsintered pattern was bumpier than that of the pattern sintered under optimal irradiation conditions (see figures 8(a), (d) and (e)).

Figure 9 shows images of the silver patterns as a function of irradiation energy. When a 3.5 J cm⁻² pulse was used, the silver pattern detached from the PET substrate due to the high light intensity (figure 9(d)).

The color of the silver nano-ink pattern changed from dark gray to yellow upon flash light sintering (figure 9).

This color change due to white light irradiation is due to the photochromism phenomenon [21, 22]. When silver nanopatterns are irradiated with white light, electrons are emitted from the nanoparticles. The emitted electrons are transferred to oxygen molecules and the silver nanoparticles become oxidized, resulting in colorless inborn silver. The silver nanopattern became yellow upon exposure to light of wavelength 420 nm, which is the wavelength at which silver nanoparticles (30–50 nm) absorb light. It should be noted that the light from the xenon lamp has a wavelength range from 390 to 900 nm (figure 1(b)) [22].

In order to compare the flash light sintered silver nano-ink with thermally sintered nano-ink, some specimens were thermally sintered in an electronic furnace. As shown in figure 10, denser necking structures were observed in the specimen sintered at 150 °C than in that sintered at 120 °C. The sheet resistance decreased as the sintering temperature increased (figure 12). However, the PET substrate was damaged when the specimen was sintered at 150 °C, as shown in the microscopy images (figure 11(b)), while the PET film of the specimen sintered at 120 °C was not damaged, as the glass transition temperature of PET is about 120 °C. In addition, the PET film of the specimen flash light sintered under optimal conditions (on-time 1.5 ms, off-time 0 ms, one

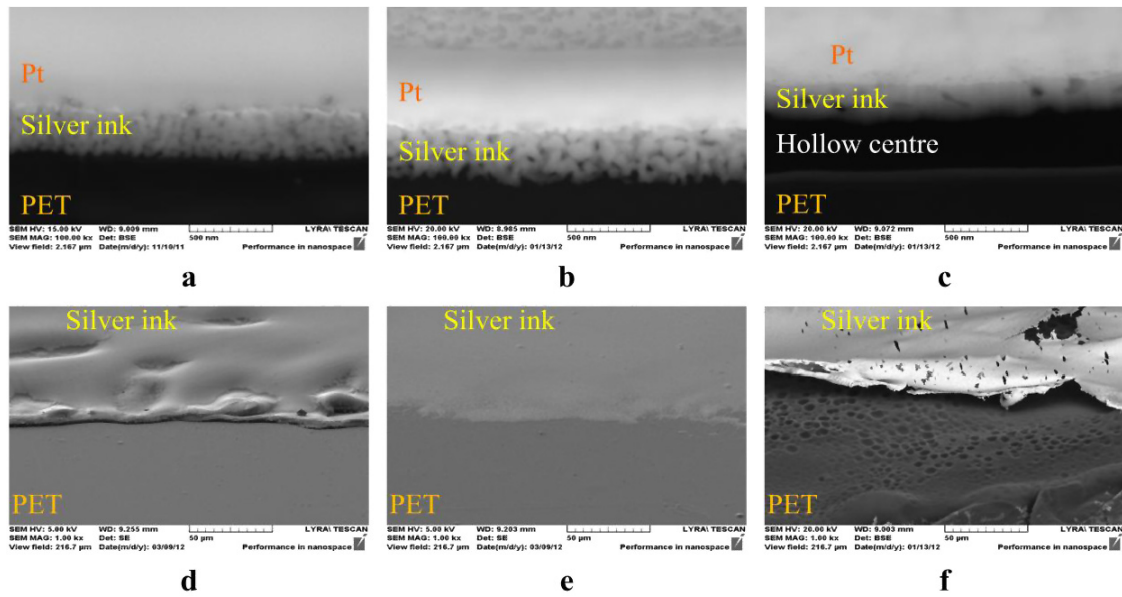


Figure 8. FIB images of energy per pulse: (a) unsintered, (b) 3 J cm^{-2} , pulse number 1, (c) 3.5 J cm^{-2} , pulse number 1, (d) unsintered (at the angle of 45°), (e) 3 J cm^{-2} , pulse number 1 (at the angle of 45°), (f) 3.5 J cm^{-2} , pulse number 1 (at the angle of 45°).

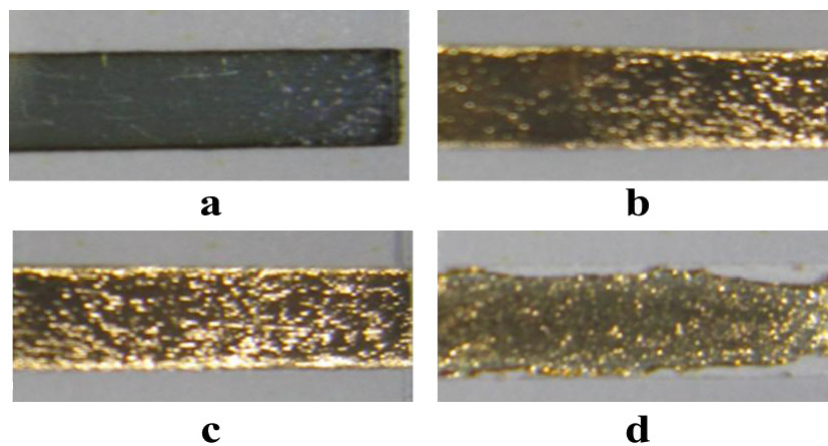


Figure 9. Digital camera images of energy per pulse: (a) unsintered, (b) 2.5 J cm^{-2} , pulse number 1, (c) 3 J cm^{-2} , pulse number 1, (d) 3.5 J cm^{-2} , pulse number 1.

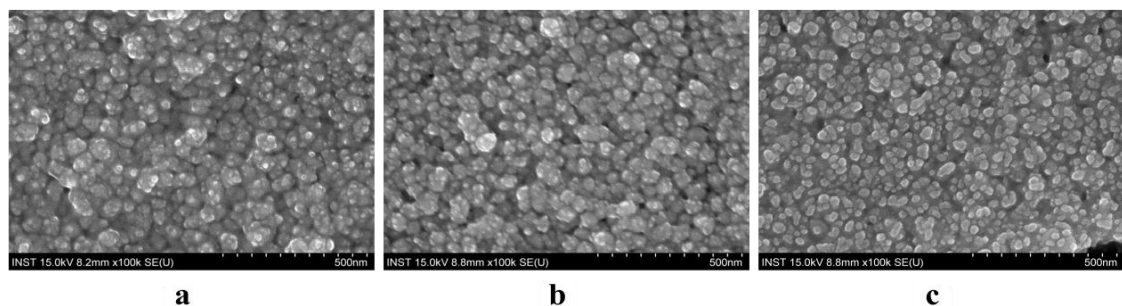


Figure 10. SEM images of thermal sintering: (a) 80°C , 1 h, (b) 120°C , 1 h, (c) 150°C , 1 h.

pulse and 3 J cm^{-2} per pulse) was not damaged. Moreover, the flash light sintered pattern shows coarser connections and larger grains among the sintered silver nanoparticles as compared with the thermally sintered pattern (see table 1(h) and figure 10(c)).

Finally, it should be noted that the silver pattern flash light sintered under optimal conditions shows a sheet resistance two times lower ($0.95 \Omega/\text{sq}$) than that of the thermally sintered pattern ($2.03 \Omega/\text{sq}$; see figure 12) without damage to the PET substrate and without interfacial delamination between the

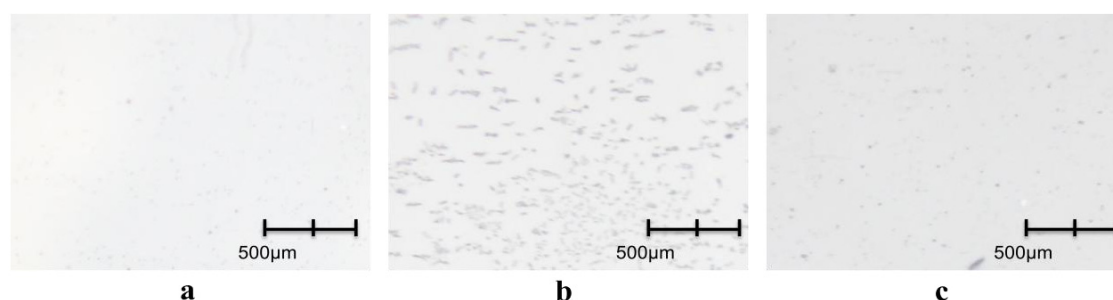


Figure 11. Microscope images of the PET substrate: (a) unsintered, (b) thermally sintered (150 °C, 1 h), (c) flash light sintered (3 J cm⁻², pulse number 1).

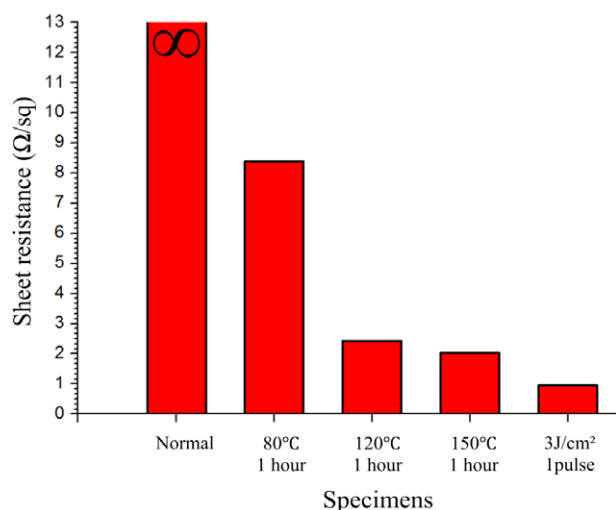


Figure 12. The sheet resistances of normal silver nano-inks, thermally sintered silver nano-inks and flash light sintered silver nano-inks.

silver film and the PET substrate. However, this is still higher than that of bulk silver films (0.01 Ω/sq). This might be due to the pores in the sintered silver film. Future work will focus on improving the quality of sintered silver films and silver nano-ink optimization.

4. Conclusion

In this study, through *in situ* monitoring of a flash light sintering process, the optimal conditions for sintering silver nanopatterns that did not damage the PET substrate were found. The optimized flash light sintering process reduced the sheet resistance of the silver film (0.95 Ω/sq) to below that of thermally sintered silver film. The *in situ* monitoring system could be used for finding the optimal sintering conditions for other metal nano-inks printed on various polymer substrates.

Acknowledgments

This work was partially supported by the Basic Science Research Program through the National Research Foundation of Korea (NRF) funded by the Ministry of Education, Science and Technology (2012-0002843). Also, this work was partially supported by the Priority Research Centers Program through the National Research Foundation of Korea (NRF)

funded by the Ministry of Education, Science and Technology (2012029029).

References

- [1] Perelaer J, de Laat A W M, Hendriks C E and Schubert U S 2008 *J. Mater. Chem.* **18** 3209–15
- [2] Khan A, Rasmussen N, Marinov V and Swenson O F 2008 *Proc. SPIE* **6879** 687910
- [3] Grouchko M, Kamyshny A, Mihailescu C F, Anghel D F and Magdassi S 2011 *ACS Nano* **5** 3354–9
- [4] Greer J R, Street R A and Materialia A 2007 *Acta Mater.* **55** 6345–9
- [5] Heng P, Seung H and Costas P G 2008 *Appl. Phys. Lett.* **93** 234104
- [6] Perelaer J, Gans B J and Schubert U S 2006 *Adv. Mater.* **18** 2101–4
- [7] Maekawa K, Yamasaki K, Niizeki T, Mita M, Matsuba Y, Terada N and Saito H 2009 *Electronic Components and Technology Conf.* pp 1579–84
- [8] Allen M L, Aronniemi M, Mattila T, Alastalo A, Ojanperä K, Suhonen M and Seppä H 2008 *Nanotechnology* **19** 175201
- [9] Ko S H, Pan H, Grigoropoulos C P, Luscombe C K, Fréchet J M J and Poulidakos D 2007 *Nanotechnology* **18** 345202
- [10] Yeo J Y, Hong S J, Lee D H, Hotz N, Lee M T, Grigoropoulos C P and Ko S H 2012 *PLoS One* **7** e42315
- [11] Kang J S, Ryu J, Kim H S and Hahn H T 2011 *J. Electron. Mater.* **40** 2268–77
- [12] Kim H S, Dhage S R, Shim D E and Hahn H T 2009 *Appl. Phys. A* **97** 791–8
- [13] Kim H S, Kang J S, Park J S, Hahn H T, Jung H C and Joung J W 2009 *Compos. Sci. Technol.* **69** 1256–64
- [14] Kang J S, Kim H S, Ryu J E, Hahn H T, Jang S H and Joung J W 2010 *J. Mater. Sci. Mater. Electron.* **21** 1213–20
- [15] Ryu J E, Kim K H, Kim H S, Hahn H T and Lashmore D 2010 *Biosens. Bioelectron.* **26** 602–7
- [16] Song Y W, Park S H, Han W S, Hong J M and Kim H S 2011 *Mater. Lett.* **65** 2510–3
- [17] Ryu J E, Kim H S and Hahn H T 2011 *J. Electron. Mater.* **40** 42–50
- [18] Lee D J, Park S H, Jang S, Kim H S, Oh J H and Song Y W 2011 *J. Micromech. Microeng.* **21** 125023
- [19] Han W S, Hong J M, Kim H S and Song Y W 2011 *Nanotechnology* **22** 395705
- [20] Park S H, Jung H M, Um S K, Song Y W and Kim H S 2012 *Int. J. Hydrog. Energy* **37** 12597
- [21] Kawahara K, Suzuki K, Ohkoy Y and Tatsuma T 2005 *Phys. Chem. Phys.* **7** 3851–5
- [22] Ohko Y, Tatsuma T, Fujii T, Naoi K, Niwa C, Kubota Y and Fujishima A 2003 *Nature Mater.* **2** 29–31
- [23] Lee T M, Noh J H, Kim I, Kim D S and Chun S 2010 *J. Appl. Phys.* **108** 102802
- [24] Kim C H, Jo J and Lee S H 2012 *Rev. Sci. Instrum.* **83** 065001